

Detailed determination of the nuclear fusion radius by a simultaneous optical model calculation of elastic scattering and fusion cross sections in reactions involving weakly bound projectiles

A. Gómez Camacho,^{1,*} P. R. S. Gomes,² J. Lubian,² E. F. Aguilera,¹ and I. Padrón³

¹*Departamento del Acelerador, Instituto Nacional de Investigaciones Nucleares, Apartado Postal 18-1027, C.P. 11801, Mexico, D.F.*

²*Instituto de Física, Universidade Federal Fluminense, Av. Litiranea s/n, Gragoatá, Niterói, R.J., 24210-340, Brazil*

³*Centro de Aplicaciones Tecnológicas y Desarrollo Nuclear (CEADEN), Playa, Ciudad de la Habana, Cuba*

(Received 6 July 2007; published 25 October 2007)

Within the optical model for direct reactions, simultaneous calculations of elastic scattering, complete fusion, and total reaction cross sections for energies around the Coulomb barrier are presented for reactions involving the weakly bound projectile ${}^9\text{Be}$ on ${}^{64}\text{Zn}$. Volume (W_F) and surface (W_{DR}) Woods-Saxon optical potentials are used such that the former is responsible only for complete fusion reactions while the latter for all direct reactions plus incomplete fusion. Simultaneous fits can be obtained with several sets of potential parameters, but if we impose the condition that the strength of W_F is smaller than the strength of W_{DR} at the tail region of the potential (this condition is discussed in detail), then values are required for r_F and r_{DR} of around 1.6 and 1.7–1.9 fm, respectively. These values are much larger than those frequently used in barrier penetration model calculations. Through the energy dependence of the real and imaginary parts of the polarization potentials, we show that the usual threshold anomaly does not show up for this system, but instead there is evidence of the presence of a breakup threshold anomaly.

DOI: [10.1103/PhysRevC.76.044609](https://doi.org/10.1103/PhysRevC.76.044609)

PACS number(s): 25.70.Jj, 24.10.-i, 24.50.+g, 25.60.-t

I. INTRODUCTION

The study of heavy ion collision mechanisms at near barrier energies has been extensively developed in the last decades. One of its main motivations is concerned with the rich interplay between different reaction processes and how they influence one another. A theoretical challenge has always been to describe simultaneously fusion, quasielastic reactions, and elastic and inelastic scattering. Discovering a unique nuclear potential that describes simultaneously different reaction mechanisms is, therefore, a goal of nuclear physicists and may be quite important for the understanding of the complexity of collision processes at low energies.

The more widely used nuclear interacting potential is the optical potential with a Woods-Saxon form for its real part and imaginary potentials corresponding to a volume part, which is responsible for the absorption of flux into the fusion channel, and a surface potential responsible for the direct reaction channels. It is well established that the energy dependences of the real and total imaginary potentials follow the dispersion relation [1,2], and that the so-called threshold anomaly (TA) [2,3] is present in most of the systems studied. It is well known that the TA is related to the decreasing behavior with the energy of the absorptive part of the nuclear polarization potential around the barrier energy. Through the dispersion relation, this fact is connected to an increase in the strength of the real part of the polarization potential just around the barrier energy.

In the late 1980s, a controversy spread in the literature concerning two different approaches for the simultaneous fit of elastic and fusion processes. Udagawa and collaborators [4–7] proposed to divide the total imaginary potential W into an inner potential W_F , responsible for fusion, such that $W_F = W$

for $r < R_F$ and $W_F = 0$ for $r > R_F$ where $R_F = r_F(A_1^{1/3} + A_2^{1/3})$ and r_F was treated as an adjustable parameter to fit simultaneously fusion and elastic scattering data. This group found that for a large variety of systems, good simultaneous fits could be obtained for r_F around 1.4 fm, corresponding to a long-range fusion potential. On the other hand, Satchler and collaborators [3,8–10] argued that a much smaller r_F could be used if the energy dependence of the optical potential due to the coupling to direct reaction channels is taken into account. In fact, this last group obtained simultaneous fits of fusion and elastic scattering, within a coupled-channels calculations approach, for a short-range fusion potential with $r_F = 1.0$ fm and diffuseness of the order of 0.25 fm.

A few years ago, a Brazilian group developed a global parameter-free optical potential known as the Sao Paulo potential (SPP) [11,12], based on the Pauli nonlocality involving the exchange of nucleons between projectile and target. Within this model, the nuclear interaction is connected with the folding potential and an extensive systematics of nuclear densities is made. This model provided good overall data description for the elastic scattering and reaction cross sections of several systems in a wide energy range [11,12]. The SPP has also been used in the description of the fusion process in the context of the barrier penetration formalism [13]. Very recently [14], it was shown that the SPP is able to predict the global behavior of fusion and reaction cross sections for hundreds of systems in a wide energy range. Extensive coupled-channels calculations were performed using the SPP as the bare potential [15,16], and reasonably good descriptions of the data were obtained for several reaction channels, without any parameter search.

Because of the availability of very high precision fusion excitation functions at near barrier energies [17–22], the concept of the simultaneous fit of elastic angular distributions, fusion, and total reaction cross sections has somehow changed. With the new high precision fusion data, one realizes that in

* agc@nuclear.inin.mx

order to fit fusion excitation functions, diffuseness parameters of the Woods-Saxon nuclear potential ranging between 0.75 and 1.5 fm are required [21,22]. These values are much larger than the usual value around 0.63 fm widely adopted to describe elastic and inelastic scattering. A possible explanation for the failure of simultaneous fits of fusion and elastic scattering [21,22] is the fact that double folding potentials are valid only in regions of very small density overlap, and therefore neither this kind of potential nor the phenomenological Woods-Saxon potential (equivalent to folding potentials at the region of the tail of the potential) can be used to describe the fusion process. The discrepancies of the fits usually can only be observed using linear scale plots of high precision fusion data, especially when plotting the derivative of the fusion cross sections as a function of energy [21,22]. Furthermore, high precision fusion excitation functions cannot be very well fitted with the same potential in the whole energy range, since different values of diffuseness are required to fit different energy regions of the excitation function [22]. However, all these discrepancies have still to be further investigated before definitive conclusions are drawn.

In the last decade, reactions involving weakly bound projectiles have become a subject of intense research [23]. Special interest has been focused on the role that the breakup coupling of such nuclei has on the fusion channel and other reaction mechanisms. Similarly, particular attention has been paid to the effect that breakup reactions have on the threshold anomaly around the Coulomb barrier. From the fact that weakly bound nuclei have small breakup threshold energies, it is expected that when these nuclei are used as projectiles, the breakup mechanisms should have a strong effect on fusion, particularly at low bombarding energies. It has recently been proposed that reactions with very weakly bound stable nuclei show a different type of anomaly called the breakup threshold anomaly (BTA) [24–26] for which, contrary to the usual threshold anomaly, the energy-dependent absorptive nuclear polarization potential does not show the tendency to decrease as the energy becomes lower around the Coulomb barrier, but rather it increases as the energy decreases. As a consequence, the corresponding real potential counterpart, which is derived from the dispersion relation, becomes repulsive and does not show the usual bell shape around the barrier energy. This breakup threshold anomaly has been suggested to be a direct consequence of the strong coupling between the elastic and breakup channels for energies around the barrier energy.

Several studies have recently been done on reactions with weakly bound projectiles such as ^9Be , ^6Li , and ^7Li on medium and heavy targets. The case of ^9Be is rather interesting, since this nucleus, being weakly bound, has no bound excited states. It is a Borromean nucleus, since once the valence neutron is removed ($E_n = -1.48$ MeV), the remaining nucleus ^8Be , being unstable, breaks up into two α particles and a neutron. Besides, due to its α - α structure, ^9Be is strongly deformed with a ground state built on a $K^{-3/2}$ rotational band. Therefore, a very interesting research subject that up to now has not been sufficiently studied is how the small neutron threshold energy and strong deformation of the ^9Be ground state intervene in determining the absence of the usual threshold anomaly.

In the present work, we analyze the available data [27–30] for scattering and reactions between the weakly bound projectile ^9Be and the medium size target ^{64}Zn and make a theoretical study of them within the direct reaction framework where optical potentials are used. A simultaneous χ^2 analysis of elastic scattering, total complete fusion, and total reaction cross sections is performed. We aim to investigate the behavior of the optical potential and the threshold anomaly for a system which involves the weakly bound projectile ^9Be and compare it with the well-known behavior for tightly bound nuclei. In the calculations, a Woods-Saxon optical potential $U_a = V_a + W_a$ for the entrance channel a is used. The imaginary part W_a is split into volume and surface parts, that is, $W_a = W_{a,F} + W_{a,DR}$. It is assumed that the volume part $W_{a,F}$ is solely responsible for the total complete fusion (TCF) process, while the surface part $W_{a,DR}$ is responsible for all other absorption processes. That is, $W_{a,F}$ accounts for the complete fusion (CF) plus the sequential complete fusion (SCF) processes. As is well known, CF is the fusion process in which the whole projectile ^9Be fuses to the target, and SCF is the fusion mechanism that results after the breakup reaction $^9\text{Be} \rightarrow \alpha + \alpha + n$, where all the fragments fuse to the target. On the other hand, $W_{a,DR}$ must include not only the elastic breakup process (EBU) in which none of the fragments is captured by the target but also the incomplete fusion mechanism. There is absorption from excited channels of the projectile and/or target, but because of the small neutron threshold energy of ^9Be and the fact that ^8Be is unstable, these contributions are regarded to be negligible. The calculated relative motion distorted waves $\chi_a^{(+)}$ obtained with the Woods-Saxon potential U_a are used throughout the calculations. In this sense, all of the calculated results are consistent with elastic scattering. The same procedure has been done previously [31] for the $^6\text{He}+^{209}\text{Bi}$ system.

An important feature of the present calculations is that we are not interested in just obtaining a simultaneous fit of elastic scattering, total reaction, and total complete fusion cross section data [27–30], but we assume that acceptable parameters of the optical potential must satisfy the condition that the strength of the fusion imaginary potential $W_{a,F}$ must be smaller than the direct reaction imaginary potential $W_{a,DR}$ at the tail region of the potentials. This assumption is supported by the following facts: (1) The works by B. T. Kim *et al.* [31] for the system $^6\text{He}+^{209}\text{Bi}$ and W. Y. So *et al.* [32] for $^6\text{Li}+^{208}\text{Pb}$ and $^9\text{Be}+^{209}\text{Bi}$ show that $|W_{a,F}| < |W_{a,DR}|$ at the strong absorption radius R_{sa} is consistently satisfied for energies around the Coulomb barrier. As a matter of fact, within the direct reaction model where fusion and direct reaction absorption processes are described by the separation of the potential W_a into $W_{a,F}$ and $W_{a,DR}$, the condition $|W_{a,F}(E, R_{sa})| < |W_{a,DR}(E, R_{sa})|$ has to be satisfied for nuclear systems that present the breakup threshold anomaly. (2) Besides the pure breakup of the projectile, which is the main component of direct reactions particularly around the barrier energy, and absorption from the excited states of the target and/or projectile, the potential $W_{a,DR}$ in this study also accounts for the incomplete fusion absorption process that is less than 10% of the total fusion cross section [30]. This fact, however, does not affect the assumption that $|W_{a,F}| < |W_{a,DR}|$ at the tail region, since the incomplete fusion process (fusion of an α particle to the target)

occurs at smaller distances where the breakup of the projectile happens.

Thus, with this condition, the simultaneous χ^2 analysis of the data reveals that the reduced radius parameters r_F and r_{DR} of the fusion ($W_{a,F}$) and direct reaction ($W_{a,DR}$) potentials take larger values than those commonly used in calculations between weakly bound projectiles with spherical targets [27, 29,33,34].

Also, in this work, the threshold anomaly is studied by the conjugate energy dependence of the fusion and direct reaction polarization potentials at the strong absorption radius R_{sa} . That is, we make a detailed analysis of the behavior of the different parts of the imaginary potential, $W_{a,F}(E)$ and $W_{a,DR}(E)$, and the corresponding real potentials $V_{a,F}(E)$ and $V_{a,DR}(E)$, which are obtained from the dispersion relation [31]. We arrive at the conclusion that for the system ${}^9\text{Be}+{}^{64}\text{Zn}$, the absorption process is dominated by the potential $W_{a,DR}$ for energies around the Coulomb barrier energy, while the total absorption potential W_a varies very slowly in this region. This is a sign that the usual threshold anomaly is not present in this system but instead the breakup threshold anomaly shows up. As a final calculation, the effect of breakup reactions (represented by $W_{a,DR}$) on complete fusion cross sections is analyzed by studying the relative effect of the potentials V_{DR} and W_{DR} on fusion. A repulsive (attractive) V_{DR} will suppress (enhance) fusion, while $W_{a,DR}$ always suppresses fusion since it represents a loss of flux from the incident channel.

II. BASIC EQUATIONS

The Schrödinger equation whose solution is the distorted-wave function $\chi_a^{(+)}$ for the problem of elastic scattering from an optical potential reads

$$(T_a + \mathcal{V}_a)\chi_a^{(+)} = E_a\chi_a^{(+)}, \quad (1)$$

with

$$\mathcal{V}_a(r, E) = V_{\text{Coul}}(r) - V_{a,0}(r) - U_a(r, E), \quad (2)$$

where $V_{\text{Coul}}(r)$ is the Coulomb potential between the reacting ions, $V_{a,0}(r)$ is the energy-independent nuclear average potential felt by the nucleons [35] and $U_a(r, E)$ is the nuclear polarization potential given by [36–38]

$$U_a(r, E) = V_a(r, E) + iW_a(r, E). \quad (3)$$

The imaginary part $W_a(r, E)$ is related to the total reaction cross section by

$$\sigma_R(E) = \frac{2}{\hbar v_a} \langle \chi_a^{(+)} | W_a(E) | \chi_a^{(+)} \rangle. \quad (4)$$

Here, v_a is the relative velocity between the colliding ions. Since the distorted-wave function can be written in expanded form as

$$\chi_a^{(+)}(k_a r) = \frac{1}{k_a r} \sum_{l_a=0}^{\infty} (2l_a + 1) \chi_{l_a}(r) P_{l_a}(\theta), \quad (5)$$

the reaction cross section can be written in the form

$$\sigma_R(E) = \frac{\pi}{k_a^2} \sum_{l_a=0}^{\infty} (2l_a + 1) T_{l_a}(E), \quad (6)$$

where the penetration factor is

$$T_{l_a}(E) = \frac{4}{\hbar v_a} \int_0^{\infty} |\chi_{l_a}(r)|^2 W_a(r, E) dr. \quad (7)$$

Now, $W_a(r, E)$ is assumed to be composed of two parts, a fusion part and the direct reaction part [31], i.e.,

$$W_a(r, E) = W_{a,F}(r, E) + W_{a,DR}(r, E), \quad (8)$$

where $W_{a,F}$ is responsible for fusion absorption and $W_{a,DR}$ for all other absorption processes. According to Eq. (3), the corresponding real polarization potentials $V_{a,F}(r, E)$ and $V_{a,DR}(r, E)$, where $V_a(r, E) = V_{a,F}(r, E) + V_{a,DR}(r, E)$, are determined by the dispersion relation [2]. The fusion (σ_F) and direct reaction (σ_{DR}) cross sections are given by equations similar to Eq. (4), where W_a should be replaced by $W_{a,F}(E)$ and $W_{a,DR}(E)$, respectively. It is important to notice that the distorted-wave function used to calculate σ_F and σ_{DR} is exactly the same as in Eq. (4); that is, $\chi_a^{(+)}$ is the solution of Eq. (1) with the full potential $U_a = V_a + iW_a$.

From now on we will drop the subindex a used above to mean the incident elastic channel. The energy-independent nuclear potential $V_0(r)$ and the fusion absorption potential $W_F(r, E)$ are assumed to have the geometrical forms

$$V_0(r) = V_0 f(r) \quad (9)$$

and

$$W_F(r, E) = W_F(E) f(r), \quad (10)$$

where

$$f(r) = \frac{1}{1 + \exp(x_i)}, \quad x_i = \frac{r - R_i}{a_i}, \quad i = 0, F. \quad (11)$$

Here a_i refers to the diffuseness parameter and $R_i = r_i(A_1^{1/3} + A_2^{1/3})$, where r_i is the reduced radial parameter. The surface imaginary potential $W_{DR}(r, E)$ is defined by

$$W_{DR}(r, E) = -4a_{DR} W_{DR}(E) \frac{df(r)}{dr}, \quad (12)$$

where a_{DR} stands for the direct reaction diffuseness and r_{DR} for the corresponding reduced radial parameter.

For the system under study, we identify the direct reaction cross section with the pure or elastic breakup plus the incomplete fusion cross sections. This is a very good approximation, because ${}^9\text{Be}$ has no excited states and its core ${}^8\text{Be}$ easily splits into two α particles. Neutron transfer is comparably less important than breakup, particularly for energies below the barrier energy. It should be pointed out that the breakup cross section may include contributions from Coulomb and nuclear interactions. This implies that the direct reaction potential includes both effects. The average potential $V_0(r)$ in Eq. (3) may have an energy dependence due to the nonlocality effect coming from a knockon-exchange contribution. However, we will not consider such effects, since they are negligible [39].

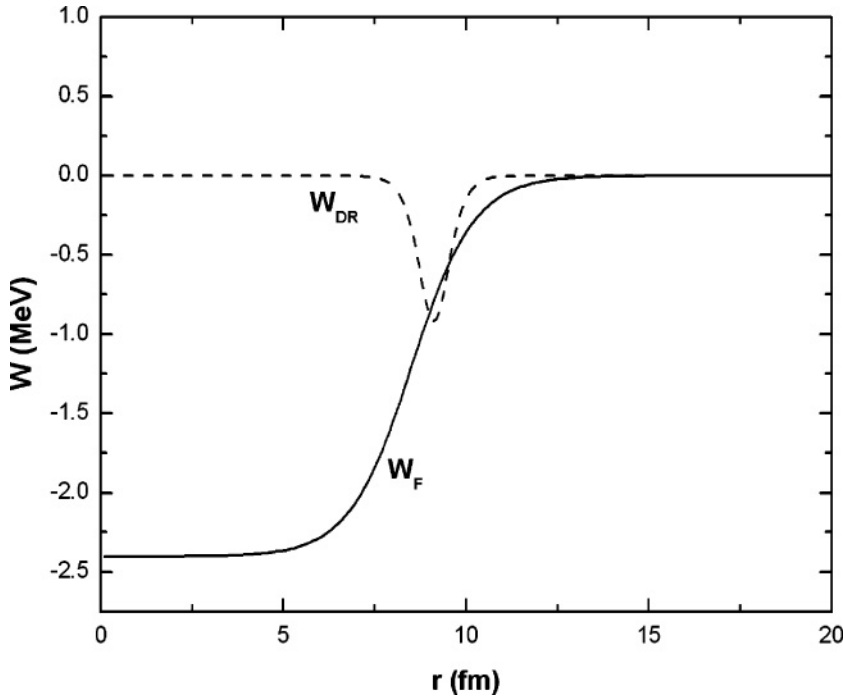


FIG. 1. Calculation of the potentials W_F and W_{DR} when the reduced radial parameters are $r_F = 1.40$ fm and $r_{DR} = 1.50$ fm, similar to those obtained by Udagawa and collaborators [4–7] for tightly bound nuclei.

III. SIMULTANEOUS χ^2 ANALYSIS OF ELASTIC SCATTERING, TOTAL REACTION, AND COMPLETE FUSION CROSS SECTIONS

In the present calculations, we consider the experimental data of Refs. [27–30] for the ${}^9\text{Be}+{}^{64}\text{Zn}$ system. We start by performing a simultaneous χ^2 analysis of elastic scattering, total reaction, and total complete fusion data at the laboratory energies of 21, 23, 26, and 28 MeV in Ref. [30]. It should be emphasized that the *derived complete fusion* cross sections given in Ref. [30] include both complete fusion and sequential complete fusion.

The Coulomb radius is set at $r_C = 1.25$ fm. Now, the optical potential parameters of the energy-independent real potential $V_0(r)$ are fixed at $V_0 = 66.0$ MeV, $a_0 = 0.52$ fm, and $r_0 = 1.22$ fm. These potential parameters are obtained by fitting elastic scattering by considering a volume Woods-Saxon absorption potential W with a fixed reduced radius $r_W = 1.4$ fm. This real nuclear potential $V_0(r)$ so defined will be kept unchanged throughout the calculations. Now, we proceed to split the absorption potential W into fusion and direct reaction parts W_F and W_{DR} and determine their parameters by means of the simultaneous χ^2 analyses of the data.

The lowest energy for which there are measurements of elastic scattering, total reaction, and complete fusion is 21 MeV, so we first tried to fit these data. In a first calculation, we used the reduced radial parameters $r_F = 1.40$ fm and $r_{DR} = 1.50$ fm, similar to those obtained by Udagawa and collaborators [4–7] for tightly bound nuclei. The agreement with the experimental fusion and total reaction cross sections is good for a large value of the diffuseness $a_F = 0.85$ fm. The W_F and W_{DR} potentials obtained in this calculation are shown in Fig. 1. One can see that these potential parameters lead to $|W_F| > |W_{DR}|$ at the tail region, which is not accepted by us as a realistic physical situation. So, in the next calculation,

we modify the values of the reduced radii r_F and r_{DR} . The simultaneous fit of the cross sections leads to the following values: $W_F = 1.498$ MeV, $W_{DR} = 0.097$ MeV, $a_F = 0.35$ fm, and $a_{DR} = 0.25$ fm, with $r_F = 1.64$ fm and $r_{DR} = 1.93$ fm, with $\chi^2/N = 0.28$. The calculated elastic scattering cross section is shown in Fig. 2(a), while the radial dependence of the potentials $W_F(r)$ and $W_{DR}(r)$ is given in Fig. 2(b). The calculated total reaction and complete fusion cross sections are $\sigma_R = 416$ mb and $\sigma_{CF} = 346$ mb. These values are very close to the measured data $\sigma_{R,\text{exp}} = 424 \pm 42$ mb and $\sigma_{CF,\text{exp}} = 344 \pm 35$ mb. Therefore, a simultaneous fit to the data has been achieved. The direct reaction cross section, which in this case corresponds to pure breakup plus incomplete fusion, is simply $\sigma_{DR} = \sigma_R - \sigma_{CF}$. From Fig. 2(b) one can see that for this parameter set, $|W_F| < |W_{DR}|$ at the tail region.

The determined values of $r_F = 1.64$ fm and $r_{DR} = 1.93$ fm are much larger than those commonly used in other optical potential calculations of reactions involving the weakly bound projectile ${}^9\text{Be}$, but they are similar to the ones obtained by Kim *et al.* [31] for the ${}^6\text{He}+{}^{209}\text{Bi}$ system, where the projectile is a halo nucleus. Since for ${}^9\text{Be}$ the optical potential calculations of neither Ref. [29] nor Ref. [34] try to calculate fusion within the same theoretical frame, the reduced radius parameters of their absorption potentials become smaller when compared with the values just determined. For instance, R. J. Woolliscroft *et al.* [34] for the system ${}^9\text{Be}+{}^{208}\text{Pb}$, used values between 1.34 and 1.37 fm for the reduced radius parameter of the absorption potential W , while Gomes *et al.* [29], for the same system studied in this work, ${}^9\text{Be}+{}^{64}\text{Zn}$, assumed values of 1.1 fm for the volume potential and 1.25 fm for the surface one. It is proposed in this paper that within the direct reaction theory as used here, larger values than those reported are required if fusion is to be calculated in conjunction with elastic scattering

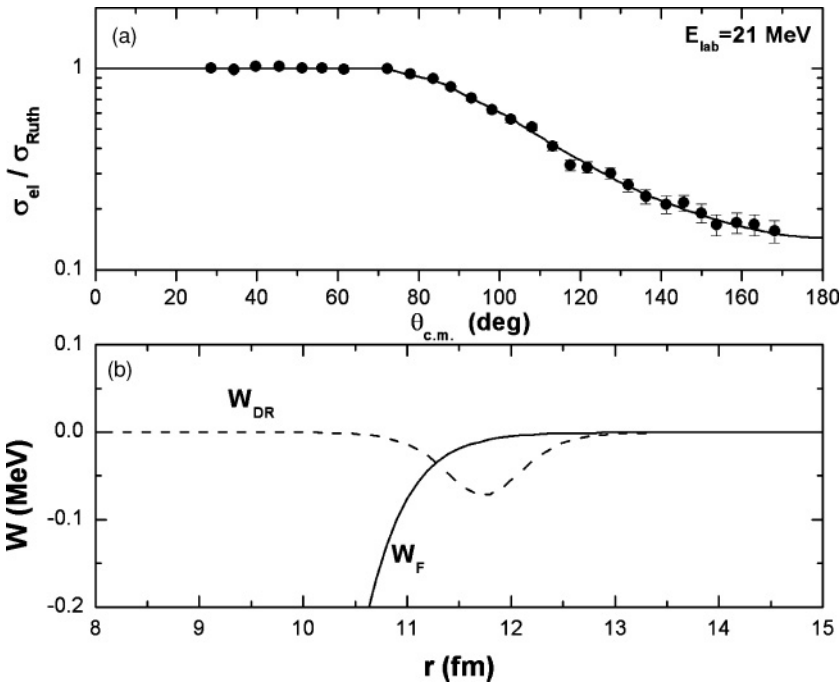


FIG. 2. Elastic scattering cross section and (b) optical potentials W_F and W_{DR} when the reduced radii are $r_F = 1.64$ fm and $r_{DR} = 1.93$ fm.

with the condition $|W_F(E)| < |W_{DR}(E)|$ for radial distances close to the strong absorption radius [40].

To show this statement, we shall make step-by-step calculations of the above-mentioned quantities, in which simultaneous fits are required for several reduced radii r_F and r_{DR} . We begin by trying to find other parameter sets for which the calculated elastic and fusion cross sections agree with the data at the same bombarding energy of 21 MeV. If the values are $r_F = 1.1$ fm and $r_{DR} = 1.25$ fm as in Ref. [27], then, W_F , W_{DR} , a_F , and a_{DR} are determined in the simultane-

ous χ^2 analysis. The following values are obtained; $W_F = 15.98$ MeV, $W_{DR} = 0.5$ MeV, $a_F = 0.862$ fm, $a_{DR} = 0.815$ fm, $\sigma_R = 421$ mb, $\sigma_{CF} = 344$ mb with $\chi^2/N = 0.42$. It is seen that the experimental values for the elastic, total reaction, and complete fusion cross sections are in good agreement with this calculation. Figure 3(a) shows the radial dependence of W_F and W_{DR} obtained by these calculations, while Fig. 3(b) presents the corresponding calculation for the elastic scattering cross section. However, one can see that although one obtains good fits to all data, these optical potential

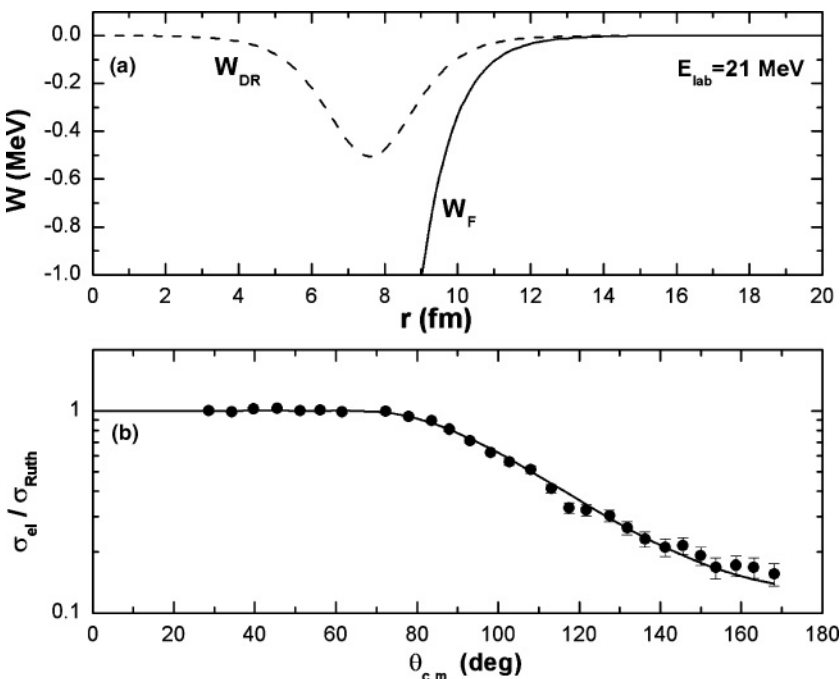


FIG. 3. Radial dependence of the potentials W_F and W_{DR} obtained with $r_F = 1.1$ fm and $r_{DR} = 1.25$ fm as in Ref. [27]. (b) Corresponding calculation for the elastic scattering cross section. The data at $E_{lab} = 21$ MeV are from Refs. [27–30].

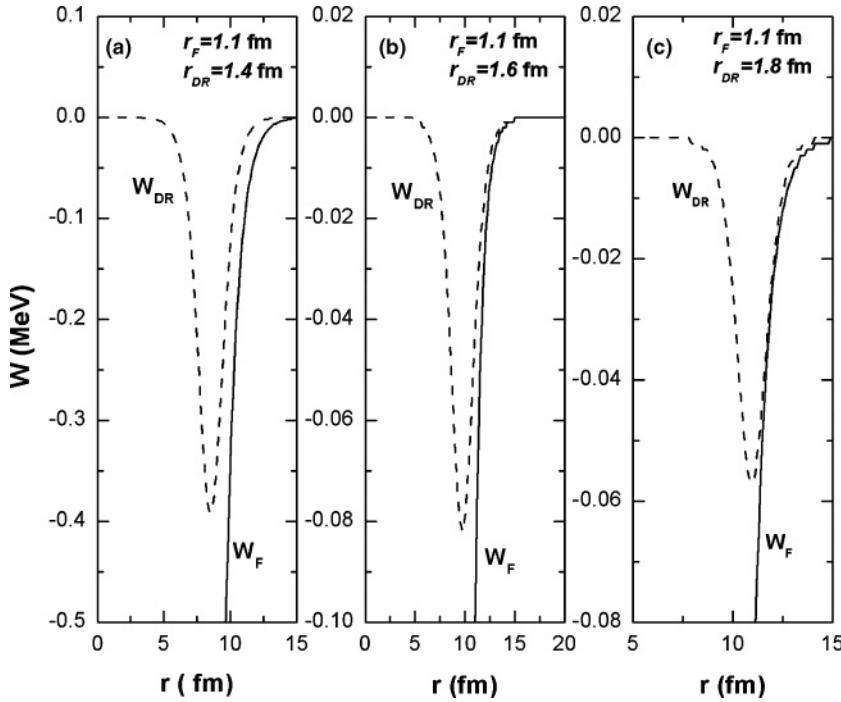


FIG. 4. Radial dependence of the optical potentials W_F and W_{DR} for three sets of r_F and r_{DR} values

parameters lead to the situation in which $|W_F| > |W_{DR}|$ for all radial distances. Therefore, as a next step, we try to increase the radial parameter r_{DR} , keeping r_F fixed at 1.1 fm in order to see whether $W_{DR}(r)$ can be pushed out of $W_F(r)$. Table I shows the results for the potential strengths, diffuseness, and the fusion and total reaction cross sections.

All these parametrizations have reasonably small χ^2/N values, and all of them fit very well the experimental elastic scattering, complete fusion, and total reaction cross sections. In Fig. 4, the radial dependence of the potentials W_F and W_{DR} are shown for the values $r_{DR} = 1.4, 1.6,$ and 1.8 fm. Figure 5 corresponds to the elastic scattering calculations. Although there are good fits to the data, all these parametrizations also lead to the situation in which $|W_F| > |W_{DR}|$, particularly at the farther tail of W_{DR} . We believed that the large values of the diffuseness a_F of the fusion potential might be largely responsible for this situation. Therefore, as a next step, we increased r_F allowing the diffuseness a_F to be reduced. Table II shows the results in which r_{DR} is kept at 1.9 fm.

TABLE I. Optical potential parameters with $r_F = 1.1$ fm. Potential strengths in MeV, diffuseness in fm, cross sections in mb.

r_{DR}	W_F	W_{DR}	a_F	a_{DR}	χ^2/N	σ_R	σ_F
1.3	17.02	0.434	0.853	0.775	0.41	421	344
1.4	16.67	0.392	0.858	0.634	0.4	421	344
1.5	9.46	0.48	0.962	0.411	0.39	423	342
1.6	35.56	0.082	0.737	0.755	0.4	420	347
1.7	39.52	0.063	0.722	0.663	0.39	419	347
1.8	39.6	0.057	0.719	0.498	0.38	419	347
1.9	3.55	0.136	1.122	0.169	0.57	424	344

As before, acceptable fits to the total reaction and fusion data are obtained; however, for the cases $r_F = 1.2$ and 1.4 fm, $|W_F| > |W_{DR}|$ in the farther tail of the W_{DR} potential as can be seen in Figs. 6(a) and 6(b). Only in the last calculation, where $r_F = 1.6$ fm and $r_{DR} = 1.9$ fm [Fig. 6(c)], we observe that $|W_F| < |W_{DR}|$ at the tail region. Corresponding elastic scattering calculations are shown in Fig. 7.

Therefore, we see that the only parametrization that simultaneously gives good predictions for the elastic scattering, complete fusion, and total reaction cross sections, and in which direct reactions start before fusion, is that where r_F and r_{DR} have values greater than 1.6 and 1.9 fm, respectively. These values are similar to the ones derived for the ${}^6\text{He} + {}^{209}\text{Bi}$ system [31]. The large values of both r_F and r_{DR} should therefore be connected to fusion and breakup reactions occurring at larger distances, probably because of the high deformation and low breakup threshold energy of the projectile; however, this point should be further investigated.

Now, we performed calculations at other energies for which complete fusion, total reaction, and elastic scattering have been measured, that is 23, 26, and 28 MeV. It should be

TABLE II. Optical potential parameters with $r_{DR} = 1.9$ fm. Potential strengths in MeV, diffuseness in fm, cross sections in mb.

r_F	W_F	W_{DR}	a_F	a_{DR}	χ^2/N	σ_R	σ_F
1.2	3.219	0.105	1.007	0.215	0.55	423	344
1.3	3.1	0.085	0.867	0.258	0.49	421	344
1.4	2.98	0.075	0.72	0.283	0.4	420	344
1.5	2.277	0.067	0.598	0.31	0.37	418	345
1.6	2.16	0.048	0.379	0.48	0.32	419	340

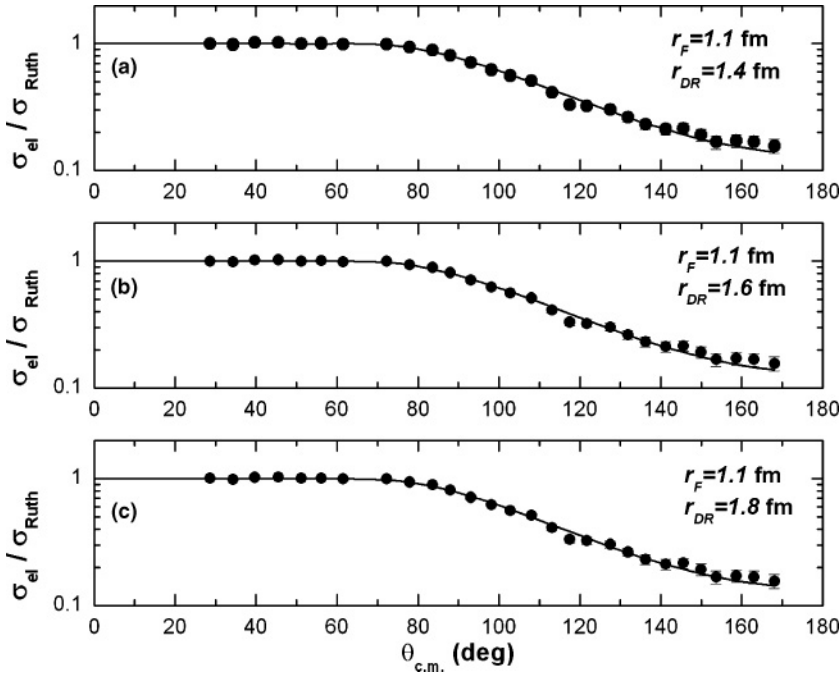


FIG. 5. Corresponding elastic scattering cross section calculations for the cases in Fig. 4. The data at $E_{lab} = 21$ MeV are from Refs. [27–30].

pointed out that because there are no available complete fusion data at 17 and 19 MeV, we estimated these by a Wong calculation [41]. By fitting the existing data at 21, 23, 26, and 28 MeV, with the parameters $V_B = 17$ MeV, $R_B = 10.0$ fm, and $\hbar\omega = 4.0$ MeV, the estimated values at 17 and 19 MeV are $\sigma_{CF} = 4.9$ and 46 mb, respectively. Table III shows the results, where the diffuseness parameters of W_F and W_{DR} have been fixed at $a_F = 0.35$ fm and $a_{DR} = 0.25$ fm as in the 21 MeV calculation. Figure 8 shows the corresponding elastic scattering calculations.

As seen in Table III, the calculated total reaction and fusion cross sections are very close to the measured values. For all the parametrizations of Table III, the condition $|W_F| < |W_{DR}|$ is satisfied in the tail region.

We inquire then about the role that the energy-independent real average potential $V_0(r)$ of Eq. (2) might play in the determination of the large values for r_F and r_{DR} . To see this, we have to redo the calculations at 21 MeV. As before, we begin by fitting the elastic scattering with a volume absorption potential W with a shorter radial parameter, say $r_W = 1.1$ fm. The parameter values obtained for $V_0(r)$ are $V_0 = 99$ MeV,

$r_0 = 1.22$ fm, and $a_0 = 0.4725$ fm; and for the absorption potential $W = 15.06$ MeV, $a_W = 0.9253$ fm. Now, we keep fixed the parameters of $V_0(r)$ and do the simultaneous fit of all the cross sections with the assumption $W = W_F + W_{DR}$, requiring that $|W_F| < |W_{DR}|$ at the tail region. We find that up to large values of r_{DR} (around 1.6 fm), close fits to the data are obtained, but still $|W_F| > |W_{DR}|$ at the tail region. We find the same behavior if $r_W = 1.2$ fm is assumed. We conclude then that a sufficiently large $r_W(r_F)$ around 1.4 fm is required so that a simultaneous fit to all the cross sections is achieved with potentials W_F and W_{DR} that satisfy $|W_F| < |W_{DR}|$ at the tail region of the potentials.

IV. STUDY OF THE THRESHOLD ANOMALY

Finally, the threshold anomaly is studied by observing the energy dependence of the potentials. This is presented in Fig. 9, where W_F and W_{DR} have been evaluated at the strong absorption radius [40] at each energy, and the strengths $V_F(E)$ and $V_{DR}(E)$ are calculated with the dispersion relation [2]. Figure 9(a) shows that V_T is strongly dominated by V_{DR} . As a matter of fact, V_{DR} becomes repulsive for energies around the Coulomb barrier energy $V_{B,c.m.} = 16.9$ MeV. On the other hand, W_{DR} increases as the energy decreases around the barrier. It has been observed that the total reaction cross section keeps appreciable values in this energy region [28–30], and in fact it is basically composed of breakup reactions, since incomplete fusion is unlikely to happen at subbarrier energies [23]. The fact that the imaginary potential increases as the energy is lowered to below the natural barrier threshold, and therefore the “threshold” ceases to be the barrier itself, was pointed out by Hussein *et al.* [24,42] as a characteristic of the breakup threshold anomaly. So, from the present results, one might say that the BTA is present for the nuclear system ${}^9\text{Be}+{}^{64}\text{Zn}$, although measurements farther below the barrier energy are

TABLE III. Optical potential parameters. Energies and strengths in MeV, radii in fm, and cross sections in mb. Data taken from Refs. [27–30]. Experimental errors are estimated at 10%.

E_{lab}	W_F	W_{DR}	r_F	r_{DR}	χ^2/N	σ_F	σ_R	$\sigma_{F,exp}$	$\sigma_{R,exp}$
17	0.552	0.096	1.55	2.03	0.9	5.0	70.0	4.9	68
19	0.465	0.23	1.54	1.87	0.68	47	190	46	199
21	1.498	0.097	1.64	1.93	0.28	346	416	344	424
23	2.9	0.185	1.57	1.7	0.39	524	603	530	590
26	2.487	0.185	1.56	1.7	0.71	774	876	800	871
28	2.36	0.11	1.58	1.74	0.74	976	1049	1000	1013

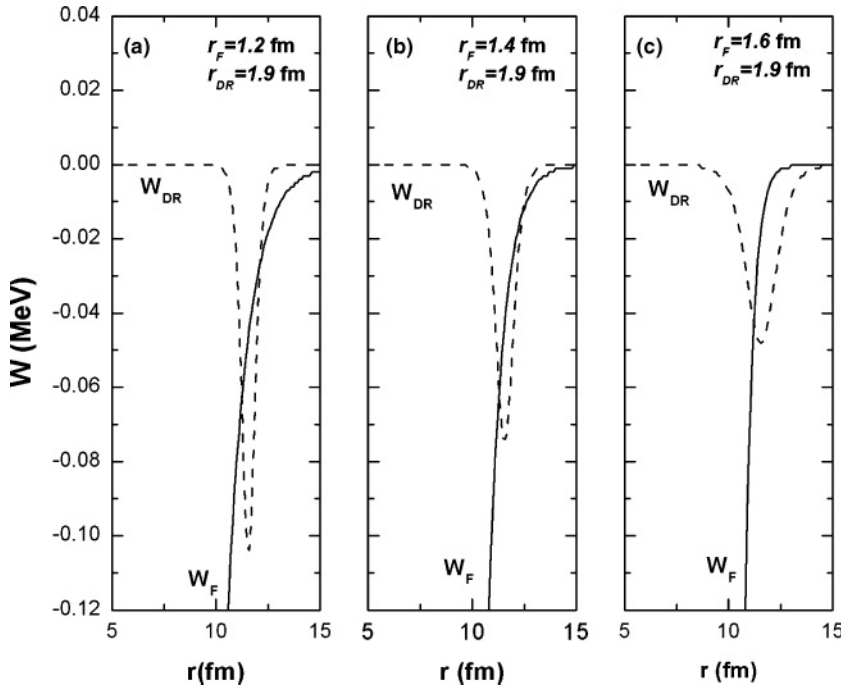


FIG. 6. Radial dependence of the optical potentials W_F and W_{DR} for three more sets of r_F and r_{DR} values.

necessary to achieve a definite conclusion. The effect of breakup coupling on fusion can be seen from Fig. 9(a). We observe that the potential V_{DR} suppresses complete fusion around the barrier energy, since this potential is repulsive in this region and consequently raises the potential barrier. On the other side, W_{DR} always represents flux absorption into reactions other than complete fusion and thus also should suppress complete fusion. We conclude that the net effect of the potentials V_{DR} and W_{DR} consists in suppressing complete fusion around the barrier energy.

V. SUMMARY

In this work, we have presented a simultaneous calculation of elastic scattering, total reaction, and complete fusion cross sections for the system ${}^9\text{Be}+{}^{64}\text{Zn}$ around the Coulomb barrier. In the model, the optical polarization potential has been split into a fusion part and a *direct reaction* part, the former is responsible for the complete fusion process, while the latter accounts for direct reaction and incomplete fusion mechanisms. A detailed step-by-step determination of the fusion and direct reaction radius parameters r_F and r_{DR} of the

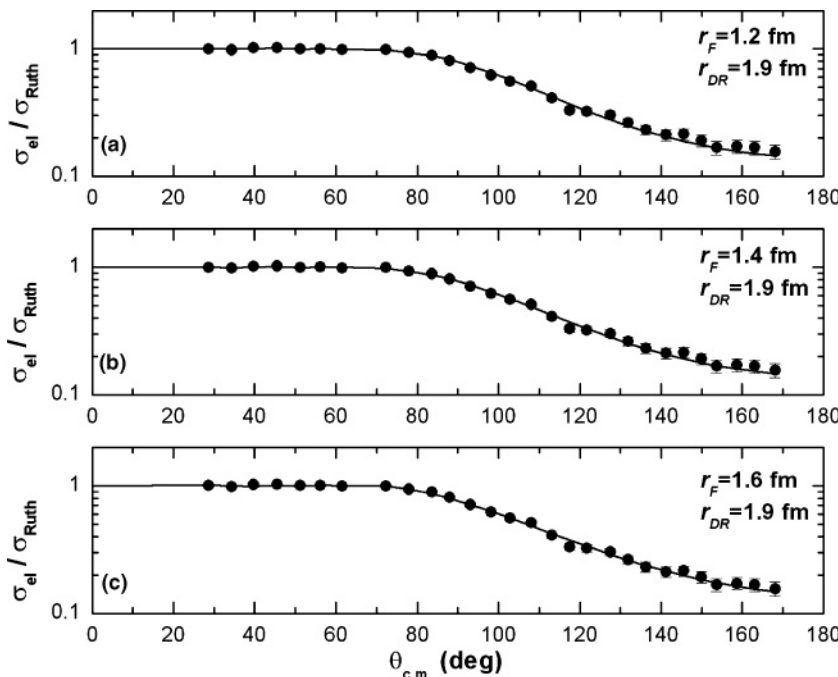


FIG. 7. Corresponding elastic scattering cross section calculations for the cases in Fig. 6. The data at $E_{lab} = 21$ MeV are from Refs. [27–30].

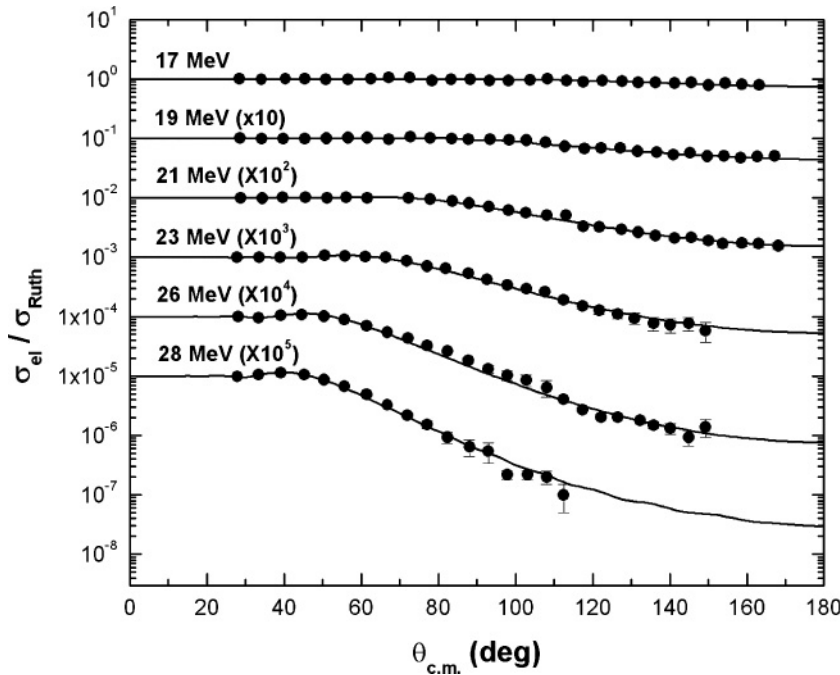


FIG. 8. Elastic scattering cross section calculations at energies of 17, 19, 21, 23, 26, and 28 MeV where the optical potential parameters are those of Table III. Data are from Refs. [27–30].

fusion and direct reaction absorption potentials is performed by a simultaneous χ^2 analysis of elastic, total reaction and complete fusion cross section data. We have shown that simultaneous fit of all data may be reached with several potential parameter sets. But, if we impose the condition that $|W_F| < |W_{DR}|$ at the tail region of the potentials, then the simultaneous fit requires that the reduced radius parameters r_F of W_F and r_{DR} of W_{DR} should take values around 1.6

and 1.9 fm, respectively. The large values of both r_F and r_{DR} are therefore connected to fusion and breakup reactions occurring at larger distances. Similar values of radii were obtained previously for the ${}^6\text{He}+{}^{209}\text{Bi}$ system, but contrary to ${}^6\text{He}$, ${}^9\text{Be}$ is not a halo nucleus, and therefore the present result is more difficult to understand.

Through the energy dependence of the polarization potential, it is concluded that the usual threshold anomaly currently

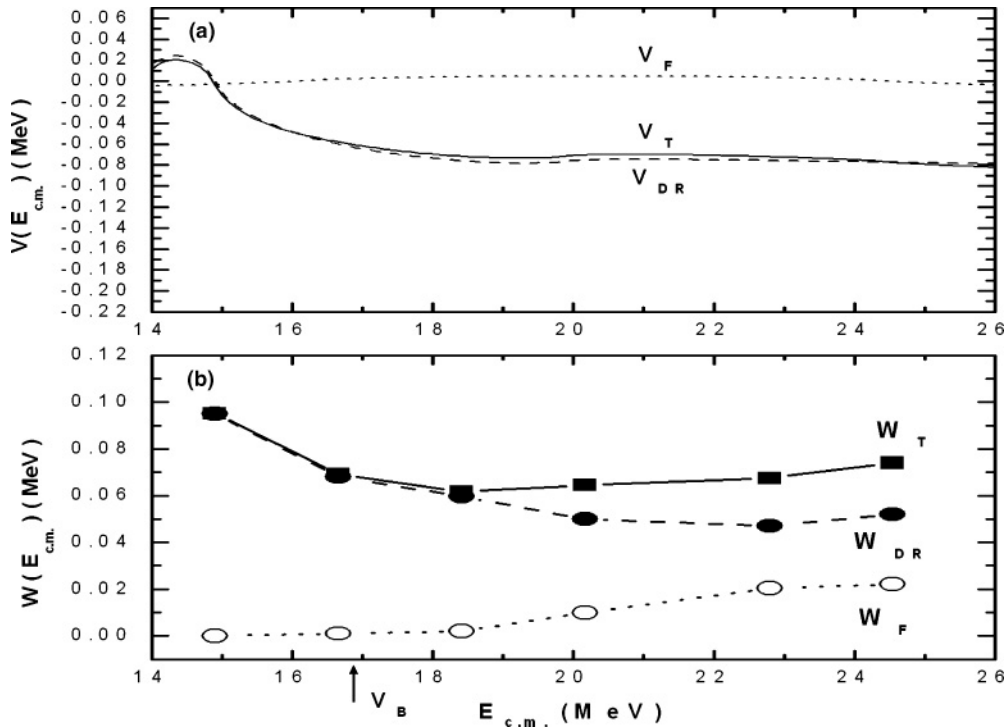


FIG. 9. Energy dependence of the nuclear polarization potential. (a) Real parts V_F , V_{DR} , and $V_T = V_F + V_{DR}$ obtained from the dispersion relation. (b) Imaginary parts W_F , W_{DR} , and W_T .

found in reactions with tightly bound nuclei is absent in the present reaction. In its place, the breakup threshold anomaly may show up, although in order to strengthen this finding, more measurements are needed below the Coulomb barrier. The effect of the surface potential V_{DR} and W_{DR} on complete fusion is found to be a net suppression around the barrier. This

is due to two effects: first, V_{DR} becomes repulsive in this region and therefore increases the height of the potential barrier; second, W_{DR} always deviates incident flux into reactions other than complete fusion. Thus, the net effect of the breakup channel coupling to complete fusion is suppression around the barrier.

-
- [1] M. A. Nagarajan, C. C. Mahaux, and G. R. Satchler, *Phys. Rev. Lett.* **54**, 1136 (1985).
- [2] C. Mahaux, H. Ngô, and G. R. Satchler, *Nucl. Phys.* **A449**, 354 (1986).
- [3] G. R. Satchler, *Phys. Rep.* **199**, 147 (1991).
- [4] T. Udagawa and T. Tamura, *Phys. Rev. C* **29**, 1922 (1984).
- [5] T. Udagawa, B. T. Kim, and T. Tamura, *Phys. Rev. C* **32**, 124 (1985).
- [6] S. W. Hong, T. Udagawa, and T. Tamura, *Nucl. Phys.* **A491**, 492 (1989).
- [7] B. T. Kim, M. Naito, and T. Udagawa, *Phys. Lett.* **B237**, 19 (1990).
- [8] M. A. Nagarajan and G. R. Satchler, *Phys. Lett.* **B173**, 29 (1986).
- [9] G. R. Satchler, M. A. Nagarajan, J. S. Lilley, and I. J. Thompson, *Ann. Phys. (NY)* **178**, 110 (1987).
- [10] I. J. Thompson, M. A. Nagarajan, J. S. Lilley, and B. R. Fulton, *Phys. Lett.* **B157**, 250 (1985).
- [11] L. C. Chamon *et al.*, *Phys. Rev. C* **66**, 014610 (2002).
- [12] M. A. G. Alvarez *et al.*, *Nucl. Phys.* **A723**, 93 (2003).
- [13] L. R. Gasques, L. C. Chamon, D. Pereira, M. A. G. Alvarez, E. S. Rossi, C. P. Silva, and B. V. Carlson, *Phys. Rev. C* **69**, 034603 (2004).
- [14] L. R. Gasques, L. C. Chamon, P. R. S. Gomes, and J. Lubian, *Nucl. Phys.* **A764**, 135 (2006).
- [15] J. J. S. Alves *et al.*, *Nucl. Phys.* **A748**, 59 (2005).
- [16] D. Pereira *et al.*, *Phys. Rev. C* **74**, 034608 (2006).
- [17] C. L. Jiang *et al.*, *Phys. Rev. Lett.* **93**, 012701 (2004).
- [18] C. L. Jiang, B. B. Back, H. Esbensen, R. V. F. Janssens, and K. E. Rehm, *Phys. Rev. C* **73**, 014613 (2006).
- [19] C. R. Morton, A. C. Berriman, M. Dasgupta, D. J. Hinde, J. O. Newton, K. Hagino, and I. J. Thompson, *Phys. Rev. C* **60**, 044608 (1999).
- [20] J. O. Newton, R. D. Butt, M. Dasgupta, D. J. Hinde, I. I. Gontchar, C. R. Morton, and K. Hagino, *Phys. Rev. C* **70**, 024605 (2004).
- [21] J. O. Newton *et al.*, *Phys. Lett.* **B586**, 219 (2004).
- [22] M. Dasgupta *et al.*, *AIP Conf. Ser.* **853**, 21 (2006); A. Mukherjee, D. J. Hinde, M. Dasgupta, K. Hagino, J. O. Newton, and R. D. Butt, *Phys. Rev. C* **75**, 044608 (2007).
- [23] L. F. Canto, P. R. S. Gomes, R. Donangelo, and M. S. Hussein, *Phys. Rep.* **424**, 1 (2006).
- [24] M. S. Hussein, P. R. S. Gomes, J. Lubian, and L. C. Chamon, *Phys. Rev. C* **73**, 044610 (2006); **76**, 049902(E) (2007).
- [25] P. R. S. Gomes, I. Padron, and J. Lubian, *J. Radiol. Nucl. Chem.* **272**, 215 (2007).
- [26] P. R. S. Gomes *et al.*, *Rev. Mex. Fis.* **S52**, 23 (2006).
- [27] S. B. Moraes *et al.*, *Phys. Rev. C* **61**, 064608 (2000).
- [28] I. Padron *et al.*, *Phys. Rev. C* **66**, 044608 (2002).
- [29] P. R. S. Gomes *et al.*, *Phys. Rev. C* **71**, 034608 (2005); **73**, 064606 (2006).
- [30] P. R. S. Gomes *et al.*, *Phys. Lett.* **B601**, 20 (2004).
- [31] B. T. Kim, W. Y. So, S. W. Hong, and T. Udagawa, *Phys. Rev. C* **65**, 044616 (2002).
- [32] W. Y. So, S. W. Hong, B. T. Kim, and T. Udagawa, *Phys. Rev. C* **69**, 064606 (2004).
- [33] R. J. Woolliscroft *et al.*, *Phys. Rev. C* **68**, 014611 (2003).
- [34] R. J. Woolliscroft, B. R. Fulton, R. L. Cowin, M. Dasgupta, D. J. Hinde, C. R. Morton, and A. C. Berriman, *Phys. Rev. C* **69**, 044612 (2004).
- [35] A. deShalit and H. Feshbach, *Theoretical Nuclear Physics*, Vol. 1 (Wiley, New York, 1974).
- [36] A. Gómez Camacho, E. M Quiroz, and T. Udagawa, *Nucl. Phys.* **A635**, 346 (1998).
- [37] A. Gómez Camacho and E. F. Aguilera, *Nucl. Phys.* **A735**, 425 (2004).
- [38] A. Gómez-Camacho, E. F. Aguilera, and A. M. Moro, *Nucl. Phys.* **A762**, 216 (2005).
- [39] G. R. Satchler and W. G. Love, *Phys. Rep.* **55**, 18 (1979).
- [40] G. R. Satchler, *Direct Nuclear Reactions* (Clarendon, Oxford, 1983).
- [41] C. Y. Wong, *Phys. Rev. Lett.* **31**, 766 (1973).
- [42] A. Gómez-Camacho, E. F. Aguilera, P. R. S. Gomes, J. Lubian, and I. Padron, *Nucl. Phys.* **A787**, 275 (2007).